

## **Contents of this file**

Figures S1 to S4

Tables S1 to S2

## **Introduction**

This supporting information consists of the following parts. Figure S1 shows spatial distributions of the emission fluxes of NH<sub>3</sub>, SO<sub>2</sub> and NO<sub>x</sub> over East Asia in summer 2010 estimated using MIX database. Figure S2 provides the comparation of the simulated SO<sub>4</sub><sup>2-</sup> and NO<sub>3</sub><sup>-</sup> concentrations in the base case and the increased emissions case. Figure S3 shows the spatial distribution of the NH<sub>3</sub> total columns in summer 2010 derived from IASI measurements. Figure S4 shows spatial distributions of WRF-Chem predicted relative humidity and precipitation in summer 2010, and the circles in Figure S4a represent the observed relative humidity obtained from NCDC dataset. Table S1 lists the options of WRF-Chem configurations. Table S2 provides the performance statistics of meteorological predictions of WRF-Chem.

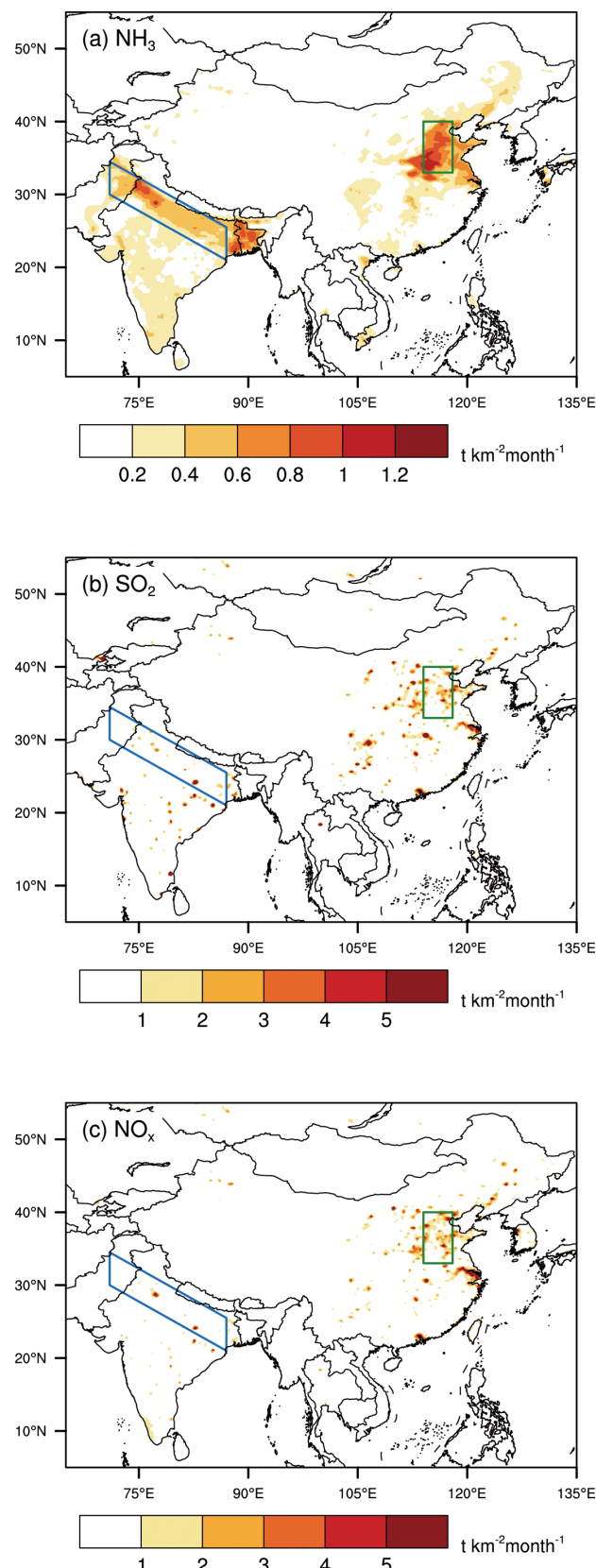


**Figure S1.** Spatial distributions of emission fluxes of (a)  $\text{NH}_3$ , (b)  $\text{SO}_2$ , and (c)  $\text{NO}_x$  over East Asia in summer 2010. The blue quadrangle represents the IGP, and the green quadrangle represents the NCP.

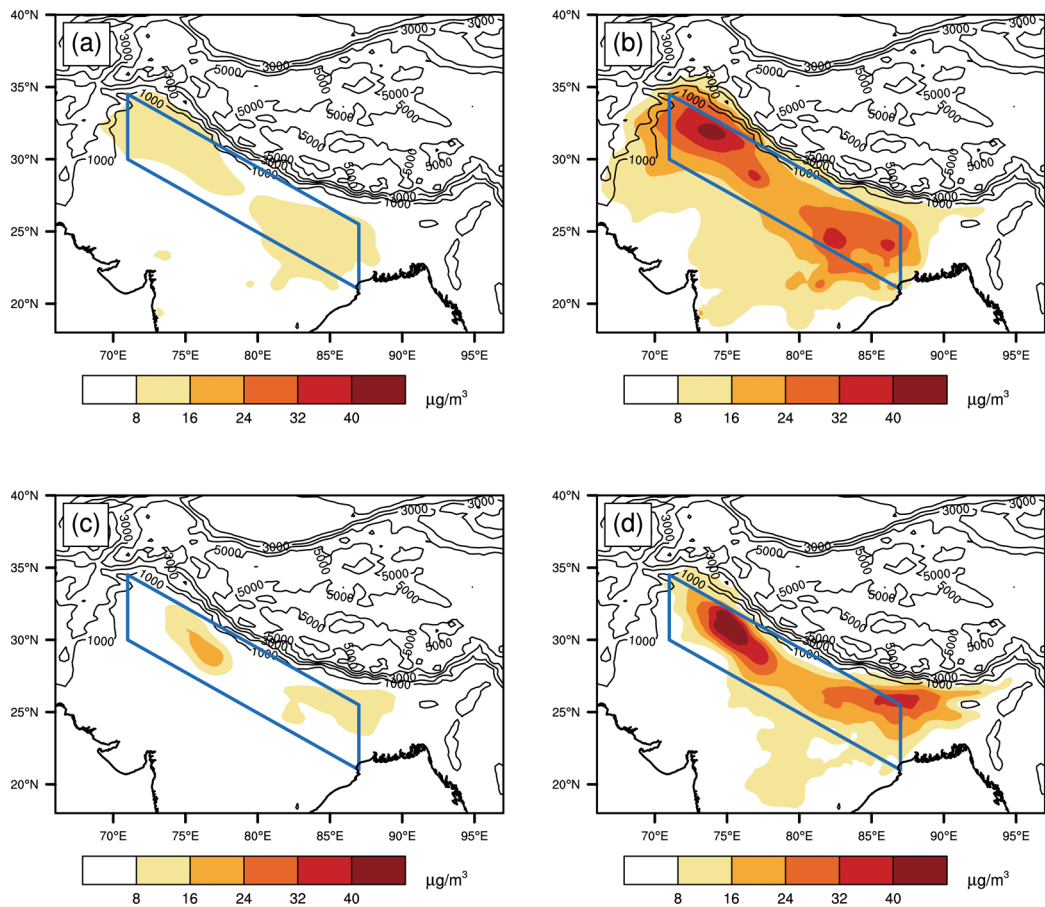


**Figure S2.** Spatial distributions of WRF-Chem predicted  $\text{SO}_4^{2-}$  and  $\text{NO}_3^-$  concentrations in summer 2010. (a) and (b) are  $\text{SO}_4^{2-}$  concentrations in the base case and the increased emissions case, respectively. (c) and (d) are  $\text{NO}_3^-$  concentrations in the base case and the increased emissions case, respectively.

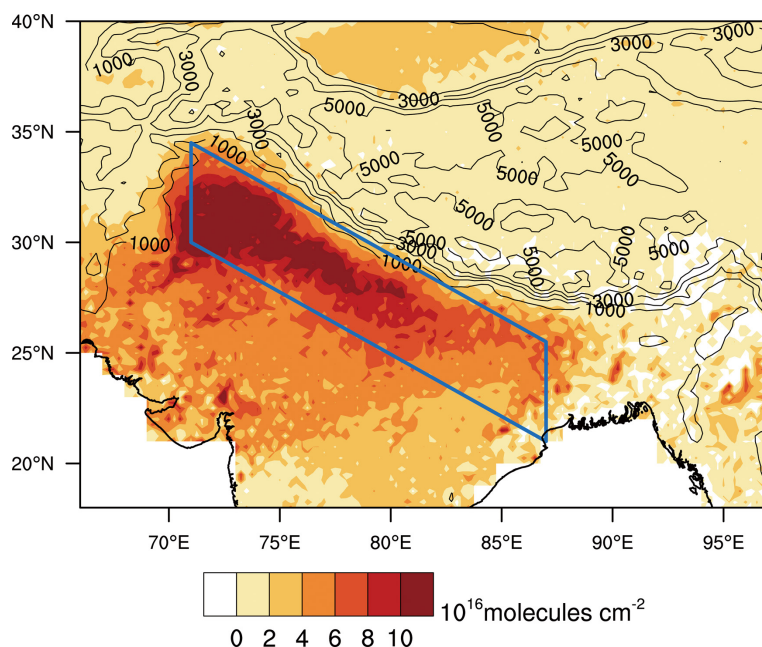


**Figure S3.** The spatial distribution of  $\text{NH}_3$  total columns in summer 2010 retrieved from IASI measurements.

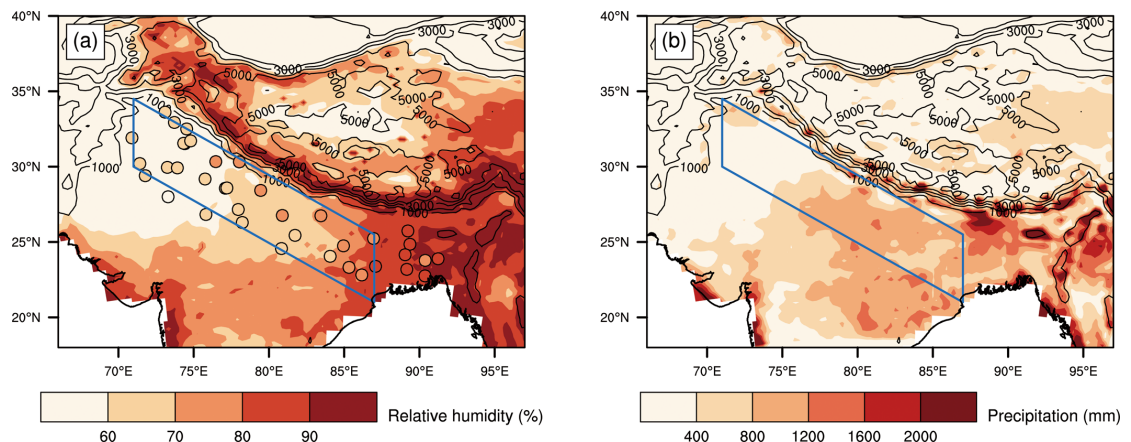


**Figure S4.** Spatial distributions of WRF-Chem predicted meteorological variables in summer 2010. (a) Relative humidity. (b) Precipitation. Circles in (a) show the observed Relative humidity.

**Table S1.** WRF-Chem configurations

Meteorology initial and boundary conditions	Reanalysis data from the National Centers for Environmental Prediction Final Analysis (NCEP-FNL)
Shortwave radiation	rapid radiative transfer model (RRTMG)
Longwave radiation	rapid radiative transfer model (RRTMG)
Land surface model	Noah land-surface model
Planetary boundary layer model	Mellor-Yamada-Janjic (Eta) TKE scheme
Cumulus parameterization	New Grell scheme (G3)
Microphysics	Lin et al. Scheme
Photolysis	Fast-J photolysis

**Table S2.** Performance statistics of meteorological predictions of WRF-Chem.

	T2 <sup>a</sup>	RH2 <sup>a</sup>	WS10 <sup>a</sup>	WD10 <sup>a</sup>
Data pairs <sup>b</sup>	27508	27443	18036	18036
MeanObs <sup>b</sup>	30.9	69.3	2.7	165.1
MeanSim <sup>b</sup>	31.9	63.3	2.9	152.9
R <sup>b</sup>	0.8	0.8	0.1	0.4
MB <sup>b</sup>	0.9	-5.9	0.2	-12.1
RMSE <sup>b</sup>	3.6	19.8	2.7	95.2
NMB (%) <sup>b</sup>	3.0	-8.6	9.1	-7.4

<sup>a</sup> T2: temperature at 2 m; RH2: relative humidity at 2 m; WS10: wind speed at 10 m; WD10: wind direction at 10 m; SLP: sea level pressure.

<sup>b</sup> data pairs: the number of observed and simulated data pairs; MeanObs: mean observational data; MeanSim: mean simulation results; R: correlation coefficient; MB: mean bias; RMSE: root mean square error; NMB: normalized mean bias.